

# Form and Skin Drag Contributions to Power Consumption for the Pitched-Blade Turbine

MIKE TAY and  
G. B. TATTERSON

Chemical Engineering Department  
Texas A&M University  
College Station, TX 77843

The determination of power consumption of rotating impellers in an agitated tank has primarily relied on traditional dimensional analysis concepts and correlations. Another traditional approach based on form and skin drag is also possible in determining the power consumption occurring in mixing. This approach, however, appears to have been neglected in the literature on mixing.

Traditionally, power number correlations for turbulent flow usually appear as

$$\frac{P_o G_c}{\rho N^3 D^5} = K \quad (1)$$

where the constant,  $K$ , is dependent on the type of impeller. Power can also be written as a drag force times a velocity:

$$P_o = F_D U \quad (2)$$

where the velocity,  $U$ , is related to impeller tip speed or  $ND$ . The drag force is usually expressed as function of a drag coefficient, the projected area (which is proportional to  $D^2$ ), fluid density, and velocity as

$$F = \frac{1}{2} C_D A \rho U^2 \quad (3)$$

The total drag force is a sum of skin and form drag forces. The force arising from skin drag is simply

$$F_{SD} = \int \tau_w dA \quad (4)$$

where  $\tau_w$  is the wall (or blade) shear stress. The force arising from form drag can be expressed as

$$F_{FD} = \Delta P A \quad (5)$$

where  $\Delta P$  is simply the pressure drop across the object or form having a projected area  $A$ . The drag coefficient in Eq. 3 incorporates both skin and form drag contributions to the drag force. The objective of this paper, in part, is to investigate the contributions of skin and form drag to the power that is transferred from a pitched-blade turbine to the fluid in mixing operations. Typically, under turbulent flow conditions, the total drag force is dominated by form drag at high Reynolds numbers.

Recent research in mixing has demonstrated the importance of vortex systems formed by the impeller blades in liquid dispersion (Ali et al., 1981) and gas dispersion (Bruijn et al., 1974; Nienow and Wisdom, 1974; Van't Riet et al., 1976). Such systems may also be important in the power transfer mechanism. In gas dispersion,

trailing vortex systems have a low pressure core that coalesces sparged gas to form gas cavities behind the impeller blades. These low-pressure vortex regions may contribute substantially to the form drag contribution of the power. The second objective of this paper is to investigate the possible interrelationship between vortex systems and power consumption for the pitched-blade turbine. This investigation includes a study of the effects of the addition of winglets and fins (added to the impeller blades in the vicinity of the vortex systems) on power consumption.

The impeller used in this study was a  $45^\circ$  pitched-blade turbine with four blades. The flows, which may be of importance, are shown in Figure 1 and exist as boundary layers on both the front and back sides of the impeller blades, a wake behind the blade, and a vortex system on the impeller blade tip. However, visual observation studies (Yuan et al., 1980) using neutrally buoyant tracer particles of the flow through the impeller indicate that the wake region behind the blade is not significant, the flow resembling a boundary layer.

For the calculation of the skin drag in this work, the boundary layers shown in Figure 1 were assumed to be turbulent on both sides of the impeller blade. It was further assumed that the boundary layers were turbulent, since the impeller Reynolds numbers indicated turbulent conditions in the tank. This, however, was not a critical assumption for the outcome of this study, and a standard correlation was used to calculate skin drag. The calculation of the form drag portion of the power required experimental determination of the pressure drop occurring across the blade.

## PRESSURE MEASUREMENTS

A hollow impeller blade was constructed out of Plexiglas with 25 pressure taps, 2.4 mm in dia., on the front and back sides of the blade, as shown in Figure 2. The pressure drop across the blade was measured using an inverted U-tube manometer mounted on the rotating impeller shaft. One side of the manometer was connected to the hollow impeller blade and to one of the 25 pressure taps on the backside of the blade. The other side of the manometer was placed directly above the impeller blade at the shaft. Pressure measurements were also made along the front of the impeller blade in a similar manner to obtain the total pressure drop across the blade.

The pressure drop measured by the manometer was corrected for centrifugal forces, since the two ends of the manometer were at two different radii, or

$$\Delta P_{\text{corrected}} = \Delta P_{\text{experimental}} - \Delta P_{\text{centrifugal}} \quad (6)$$

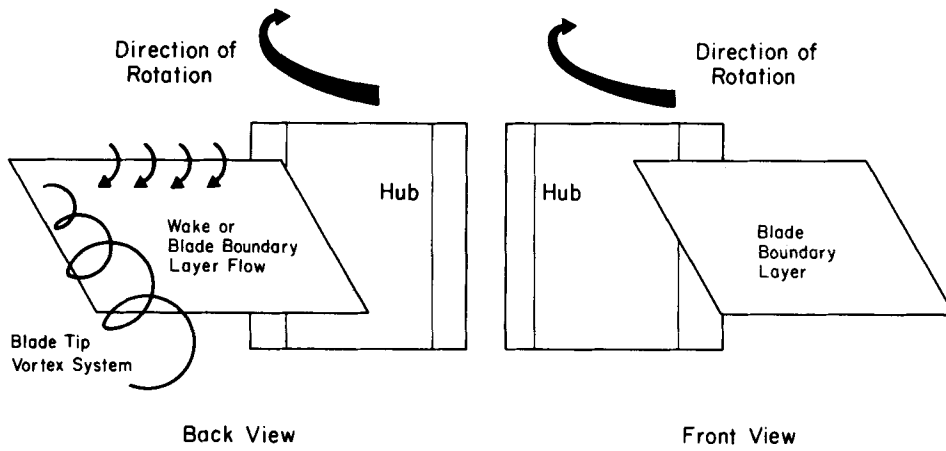


Figure 1. Flow generated by the pitched-blade turbine.

where  $\Delta P_{\text{centrifugal}}$  was obtained from

$$\Delta P_{\text{centrifugal}} = \int_{r_1}^{r_2} \frac{\rho}{g_c} \frac{U^2}{r} dr \quad (7)$$

and  $U = 2\pi Nr$ . The corrected pressure drop measurements were rearranged in terms of a pressure coefficient:

$$C_p = \frac{\Delta P_{\text{corrected}}}{\frac{1}{2} \rho U_{\text{impeller tip speed}}^2} \quad (8)$$

#### EXPERIMENTAL EQUIPMENT

The impeller used in the study was 45° pitched-blade turbine, 304.8 mm in dia., with four blades 72.4 mm in width. The turbine was mounted 300 mm from the tank bottom along the centerline of a transparent Plexiglas tank. The 900 mm dia. cylindrical mixing tank was filled with water to a height 900 mm. Four baffles, 91 mm in width, were placed symmetrically on the wall inside the cylindrical tank. A Chemineer 2HTD-Z 2 hp agitator with variable speed drive up to 350 rpm was used for the study. Pressure measurements were performed at impeller rotational speeds of 2 and 4 s<sup>-1</sup>.

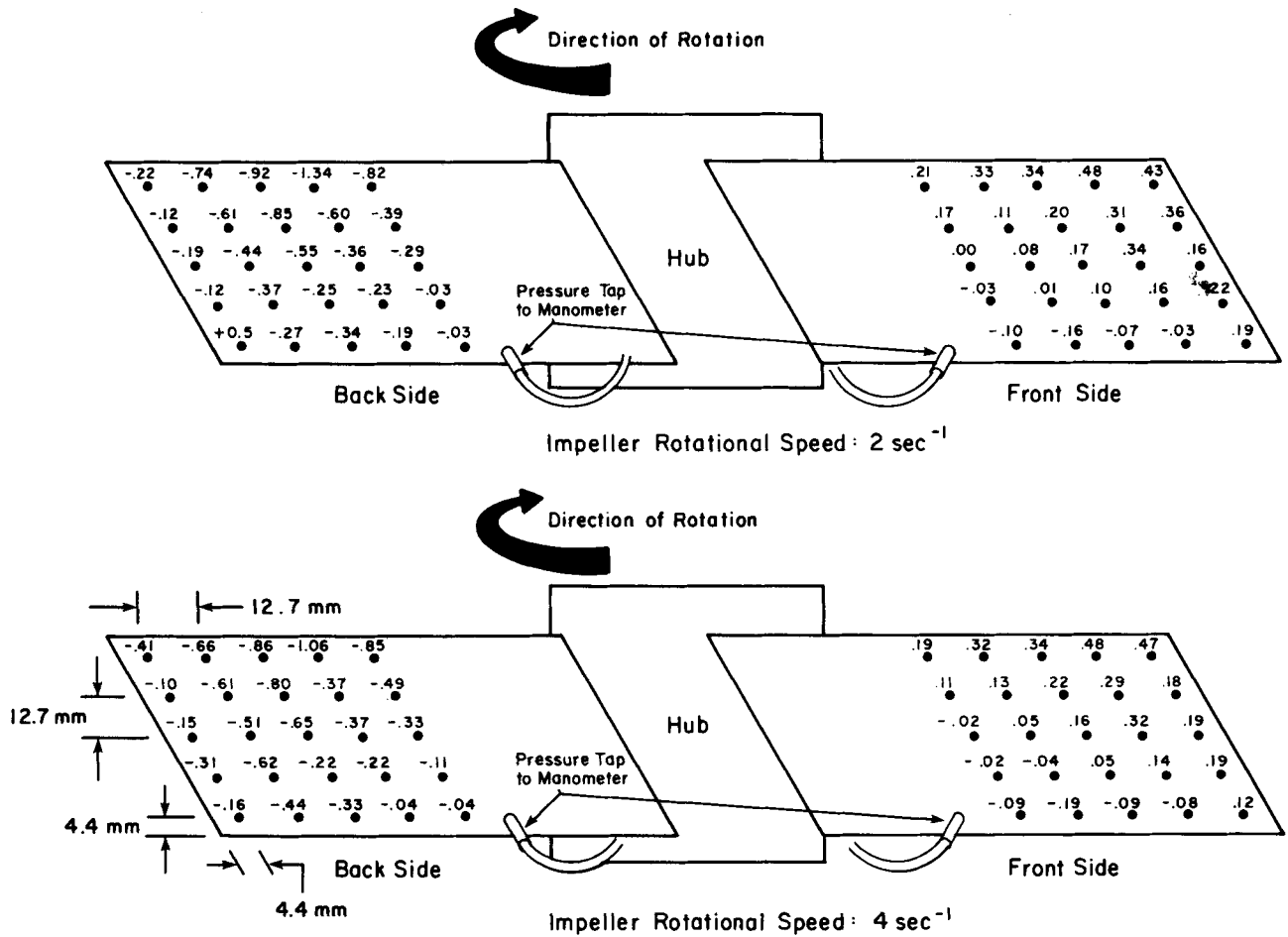


Figure 2. Pressure coefficients as a function of blade position and impeller rotational speed.

Name	Blade Geometry		Power Number
	Side View	Top View	
Normal Blade Geometry			.79
Winglet			.83
Extended Winglet			.97
Top Fin			1.12
Middle Fin			.79
Bottom Fin			.77

Figure 3. Power numbers and impeller blade geometries.

Various winglets and fins were added to the impeller, as shown in Figure 3. A Valenite Power Monitor was used to measure the power consumed in mixing for the various geometries studied.

## RESULTS AND DISCUSSION

The power numbers, obtained from the power meter measurements, for the various geometries of the pitched-blade turbine with winglets and fins are listed in Figure 3, as well as the power number for a normal pitched-blade turbine. A power number of 1.37 for a normal six-bladed, 45° pitched-blade turbine has been reported previously (Bates et al., 1963). Since power is proportional to blade number, the power number of 1.37 scales to 0.9 for a normal

four-pitched-blade turbine, which is in agreement with our data. As observed in Figure 3, only the extended winglet and top mounted fin geometry caused an effect on the power consumption over that of a normal pitched blade turbine. The other blade geometries had little effect on power consumption.

The skin drag force on the impeller blade (Bober and Kenyon, 1980) was calculated approximately using the following correlation:

$$F_{SD} = .036 \frac{\rho U_{local}^2 b L}{g_c} \left( \frac{v}{U_{local} L} \right)^2 \quad (9)$$

where  $U_{local}$  was varied between the impeller tip speed and the impeller hub velocity. Power consumption, consumed in skin drag, was then calculated using Eq. 10.

**TABLE 1. POWER NUMBERS OBTAINED FROM SKIN AND FORM DRAG**

Reynolds No.	Impeller		Power due to			Power No.
	Rotational Speed, $s^{-1}$		Skin Drag W	Form Drag W	Total Drag Force, W	
2.0	2		0.40	20.6	21.0	1.00
4.0	4		2.71	165	168	1.00

$$P_o = F_{SD}U_{local} \quad (10)$$

Table 1 lists the power necessary for skin drag for the entire impeller for the two rotational speeds, 2 and 4  $s^{-1}$ .

The local pressure coefficients, determined experimentally, are listed in Figure 2 for the front and back sides of the blade for impeller rotational speeds of 2 and 4  $s^{-1}$ . Positive coefficients indicated a pressure increase; negative coefficients, a pressure drop. The pressure coefficients nearer the hub drop off rapidly to zero. The form drag force was then calculated using Eq. 5 and the pressure coefficients. The power consumed in the form drag, shown in Table 1, was calculated using Eq. 11 where the summation was over the blade sections:

$$P_o \text{ per blade} = \sum \frac{C_{p \text{ local}} A \rho U_{\text{tip scale}}^2}{2g_c} U_{\text{local}} \quad (11)$$

where

$$C_{p \text{ local}} = (C_{P \text{ backside}} + C_{P \text{ frontside}})_{\text{local}} \quad (12)$$

and where  $U_{\text{local}}$  varied according to the location of the blade sections. If the power distributions in Eq. 11 were projected back to the impeller hub region, the power consumed in form drag in Table 1 would have increased by 10%.

The power numbers, which include the power consumed in form and skin drag for the two rotational speeds, are listed Table 1. Form drag of the impeller obviously dominated the power consumption for the pitched-blade turbine, as shown in Table 1. This was not unexpected but has not been clearly demonstrated in the literature on mixing. Furthermore, the low pressure regions of the vortex systems do not contribute to the form drag portion of the power consumption. The pressure coefficients in Figure 2 shows no evidence of the vortex structure and the pressure coefficients were distributed uniformly over the impeller blade. The fact that form drag controls the power consumption also explains why winglets and fins, added to impeller blades to change the behavior of the vortex systems, did not significantly affect the power consumption.

The extended winglet and top fin blade geometries affected power consumption by changing the form drag of the impeller blade.

#### NOTATION

$A$	= projected area
$b$	= boundary-layer width
$C_D$	= drag coefficient
$C_P$	= pressure coefficient
$D$	= impeller diameter
$F_D$	= drag force
$F_{FD}$	= form drag
$F_{SD}$	= skin drag
$g_c$	= gravitational constant
$K$	= constant
$L$	= boundary-layer length
$N$	= impeller rotational speed
$P_o$	= power
$\Delta P$	= pressure drop
$r$	= radius
$U$	= velocity
$\rho$	= density
$\tau_w$	= wall shear stress
$\nu$	= kinematic viscosity

#### LITERATURE CITED

- Ali, A. M., et al., "Liquid Dispersion Mechanisms in Agitated Tanks. I: Pitched-Blade Turbine," *Chem. Eng. Commun.*, **10**, 205 (1981).
- Bates, R. L., P. L. Fondy, and R. R. Corpstein, "An Examination of Some Geometric Parameters of Impeller Power," *Ind. Eng. Chem. Process Des. Dev.*, **2**, 4, 310 (1963).
- Bober, W., and R. A. Kenyon, *Fluid Mechanics*, Wiley, New York, 469 (1980).
- Bruijn, W., K. Van't Riet, and J. M. Smith, "Power Consumption with Aerated Rushton Turbines," *Trans. Inst. Chem. Eng.*, **52**, 88 (1974).
- Nienow, A. W., and D. J. Wisdom, "Flow over Disc Turbine Blades," *Chem. Eng. Sci.*, **29**, 1,994 (1974).
- Van't Riet, K., J. M. Boom, and J. M. Smith, "The Behavior of Gas-Liquid Mixtures Near Rushton Turbine Blade," *Trans. Inst. Chem. Eng.*, **54**, 124 (1976).
- Yuan, H. H. S., R. S. Brodkey, and G. B. Tatterson, "Stereoscopic Visualization of the Flows for Pitched Blade Turbines," *Chem. Eng. Sci.*, **35**(6), 1,369 (1980).

*Manuscript received June 28, 1984; revision received Nov. 13 and accepted Nov. 24, 1984.*